Impact of the Indian Ocean SST basin mode on the Asian summer monsoon

Jianling Yang,[1] Qinyu Liu,[1] Shang-Ping Xie,[1,2] Zhengyu Liu,[1,3] and Lixin Wu[1]

Received 25 October 2006; revised 26 November 2006; accepted 13 December 2006; published 26 January 2007.

[1] Following an El Niño event, a basin-wide warming takes place over the tropical Indian Ocean, peaks in late boreal winter and early spring, and persists through boreal summer. Our observational analysis suggests that this Indian Ocean warming induces robust climatic anomalies in the summer Indo-West Pacific region, prolonging the El Niño's influence after tropical East Pacific sea surface temperature has returned to normal. In response to the Indian Ocean warming, precipitation increases over most of the basin, forcing a Matsuno-Gill pattern in the upper troposphere with a strengthened South Asian high. Near the ground, the southwest monsoon intensifies over the Arabian Sea and weakens over the South China and Philippine Seas. An anomalous anticyclonic circulation forms over the subtropical Northwest Pacific, collocated with negative precipitation anomalies. All these anomaly patterns are reproduced in a coupled model simulation initialized with a warming in the tropical Indian Ocean mixed layer, indicating that the Indian Ocean warming is not just a passive response to El Niño but important for summer climate variability in the Indo-West Pacific region. The implications for seasonal prediction are discussed. **Citation:** Yang, J., Q. Liu, S.-P. Xie, Z. Liu, and L. Wu (2007), Impact of the Indian Ocean SST basin mode on the Asian summer monsoon, *Geophys. Res. Lett.*, *34*, L02708, doi:10.1029/2006GL028571.

1. Introduction

[2] El Niño/Southern Oscillation (ENSO) is the dominant mode of climate variability on the instrumental record, exerting profound influences on climate around the globe. During a typical El Niño event, sea surface temperature (SST) anomalies in the equatorial Pacific peak around December and decay rapidly in the following boreal spring (hereafter, seasons refer to those for the Northern Hemisphere). El Niño's influences persist into the next summer, one season after Pacific SST anomalies are gone, in circulation and rainfall anomalies in South and East Asia [*Yang and Lau*, 1998; *Kawamura*, 1998; *Huang et al.*, 2004], the South China Sea [*Xie et al.*, 2003] the tropical Northwest Pacific [*Wang et al.*, 2003], the Indian Ocean [*Reason et al.*, 2000], and the zonal-mean upper-tropospheric geopotential height [*Kumar and Hoerling*, 2003; *Lau et al.*, 2005].

[3] The present study investigates the role of the Indian Ocean in prolonging the ENSO influence into summer, focusing on the Asian monsoon region. In response to an El Niño, the Indian Ocean displays a basin-wide warming that peaks in late winter and persists into the following spring and summer (Figure 1). This Indian Ocean basin mode (IOBM) is the dominant mode of SST variability in the basin, forced by ENSO-induced heat flux anomalies [*Klein et al.*, 1999] except in the tropical South Indian Ocean where ocean Rossby waves are an important mechanism for SST variability [*Xie et al.*, 2002]. Note that the IOBM is defined here as a mode of SST variability and different from the basin modes of ocean wave adjustment. Recent model studies suggest an IOBM feedback on the growth and decay of ENSO [*Wu and Kirtman*, 2004; *Annamalai et al.*, 2005a, 2005b; *Kug et al.*, 2006]. Our observational analysis extends these studies by showing that the IOBM influence persists into summer, characterized by a Matsuno-Gill pattern in the upper troposphere and a low-level anticyclonic pattern over the subtropical Northwest Pacific. Our coupled model experiment further demonstrates that these patterns are indeed induced by IOBM SST anomalies.

[4] The rest of the paper is organized as follows. Section 2 describes the datasets and methods. Sections 3 and 4 present results from the observational analysis and model experiment, respectively. Section 5 is a summary.

2. Data and Methods

[5] We use monthly geopotential height at 200 hPa and 850 hPa (hereafter H200 and H850, respectively), wind velocity at 850 hPa, and precipitation derived from the National Centers for Environmental Prediction/National Center for Atmospheric Research (NCEP/NCAR) reanalysis, and SST come from the monthly Hadley Center sea ice and SST data set (HadISST), for the 55-year period of 1950–2004. Interannual anomalies are defined as deviations from the monthly climatology. A third-order polynomial is subtracted from the 55-year time series by a least square fit to remove the trend and multi-decadal variability. The 95% significance level for correlation is 0.38 for a student-t test if we assume a decorrelation timescale of two years, a reasonable choice for ENSO.

[6] The Nino3 index is defined as SST anomalies averaged over the eastern equatorial Pacific (5°S–5°N, 150°W–90°W), and the IOBM index as the time series of the first empirical orthogonal function (EOF)

[1] Physical Oceanography Laboratory, and Ocean-Atmosphere Interaction and Climate Laboratory, Ocean University of China, Qingdao, China.
[2] International Pacific Research Center and Department of Meteorology, University of Hawaii, Honolulu, Hawaii, USA.
[3] Center for Climatic Research, University of Wisconsin, Madison, Wisconsin, USA.

0094-8276/07/2006GL028571$05.00

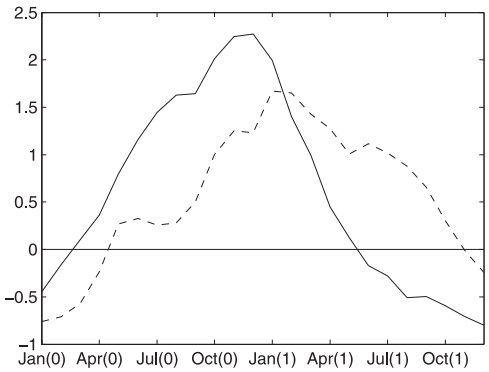

Figure 1. Evolution of a composite El Niño event: the Nino3 (solid) and IOBM (dashed) indices normalized by their respective annual-mean standard deviations. Numerals "0" and "1" denote years during which El Niño develops and decays, respectively.

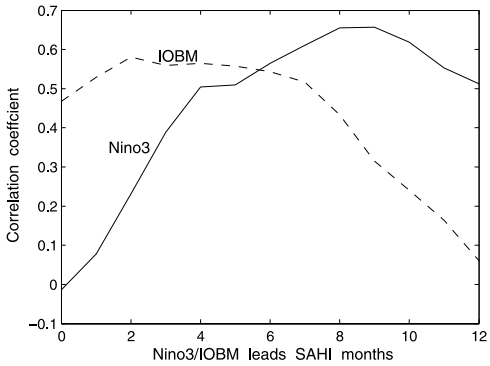

Figure 3. Correlation with the Jul/Aug(1) South Asian high index: the Nino3 (solid) and IOBM (dashed) indices, as a function of the time in months by which Nino3/IOBM leads.

mode of SST variability over the tropical Indian Ocean (40–110°E, 20°S–20°N).

3. IOBM Effects in Summer

[7] Figure 1 shows the composites of the normalized Nino3 (solid) and IOBM (dashed) indices of the Indian Ocean from 14 El Niño events (1951, 1957, 1963, 1965, 1969, 1972, 1976, 1982, 1986, 1987, 1991, 1994, 1997, 2002), in which the Nino3 index exceeds 0.75 standard deviation for consecutive three months of Nov(0)-Jan(1). Here "0" and "1" in parentheses denote the developing and decay years of ENSO, respectively. ENSO displays a strong seasonality: a typical El Niño develops in summer and fall, peaks in early winter, and decays rapidly in late winter and the following spring. The Indian Ocean warming lags by one to two seasons, developing in fall and peaking in late winter and spring. The IOBM index persists through the summer and reverses the sign in Nov(1). In Aug(1), the IOBM index stands at half of its peak value in Jan/Feb(1). Of particular relevance to this study, the IOBM's persistence makes it a viable candidate to prolong ENSO's influences after Pacific SST anomalies have dissipated. The La Nina composites are similar except for a sign difference, with the IOBM lagging and persisting into the summer (not shown).

3.1. Upper Tropospheric Circulation

[8] Figure 2 shows the IOBM's influence on the upper tropospheric circulation as represented by correlation of SST and H200 in Apr/May(1) and Jul/Aug(1) with the Apr(1) IOBM index. Apr(1) is chosen since it is the time when the Nino3 index has decreased to less than 20% of the Nov/Dec(0) peak while the IOBM index remains high at 80% of the Jan/Feb(1) maximum (Figure 1). In Apr/May(1), high H200 correlation (>0.8) occupies the entire equatorial belt while SST anomalies are positive in all three tropical oceans.

[9] One season later in Jul/Aug(1), SST anomalies weaken in magnitude but remain positive over most of the Indian Ocean except off the Somali coast, where an intensified Findlater wind jet causes a SST cooling via upwelling as will be seen shortly. Besides a general decrease in magnitude, the H200 correlation with the Apr(1) IOBM index changes considerably in spatial structure. Instead of being zonally uniform, summer H200 anomalies are highly asymmetric in the east-west direction. High correlation ($\geq$0.6) is found in the subtropics on either side of the equator west of the 80°E while it is trapped on the equator to the east over the Maritime Continent, reminiscent of the Rossby and Kelvin response of *Gill* [1980] to a tropical heating centered on the equator, respectively. Along the equator, H200 correlation reaches a meridional maximum east of 90°E but a meridional minimum to the west, an east-west asymmetry due to the eastward propagation of the Kelvin wave forced by a zonally confined heat source over the tropical Indian Ocean. The drastic changes in H200's spatial structure from spring to summer are likely due to the diminished SST/precipitation anomalies over the tropical Pacific or the interaction with mean flow changes. It can also be caused by the onset of the climatological mean southwest monsoon wind which transports the anomalous

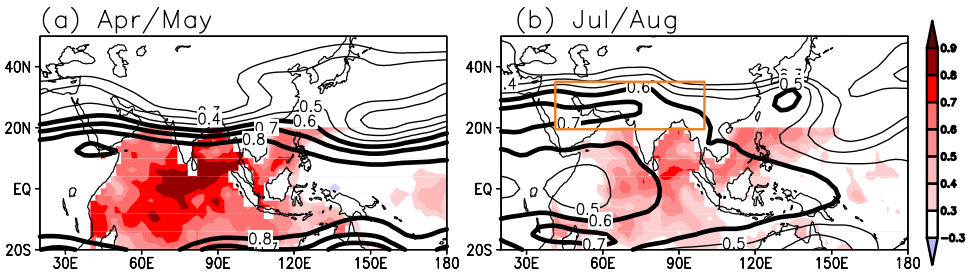

Figure 2. Correlation with the Apr(1) IOBM index during (a) Apr/May(1) and (b) Jul/Aug(1): SST (color) and geopotential height at 200 hPa (thick contours $\geq$ 0.6). The orange box denotes the region for the SAH index definition.

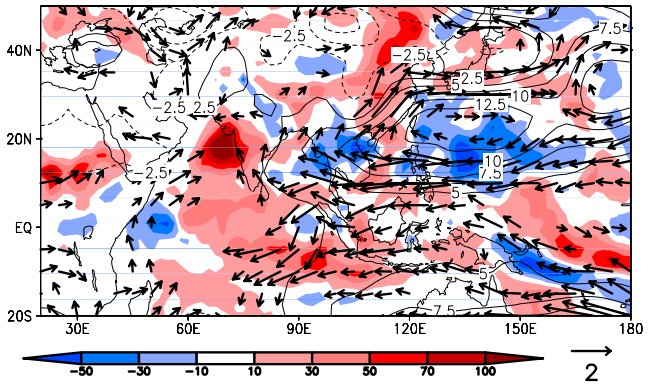

Figure 4. Composite differences for Jul/Aug(1) between IOBM warm and cold events: precipitation (color in mm/month), geopotential height (contours in m), and wind velocity (vectors in m s^{-1}) at 850 hPa.

water vapor into the South Asia, forming an additional heating source [*Liu et al.*, 2006].

[10] Figure 3 shows the lagged correlations with the Nino3 and IOBM indices of Jul/Aug(1) H200 averaged in 40–100°E, 20–32.5°N, an index we use to measure the strength of the South Asian High (SAH), which forms during the summer monsoon. The Nino3 and SAH indices are not correlated at lag 0 but their correlation increases with the lag and peaks with the former leading by 7–10 months [equivalent to Oct-Dec(0) for Nino3]. Thus, ENSO affects the summer SAH, but not directly. Instead, it needs some other mechanisms to relay its influence to summer. The ENSO-induced IOBM is such a mechanism, indeed correlated significantly with the SAH index at lag 0. The IOBM-SAH correlation increases slightly with the former leading by 2–6 months, suggesting that other processes such as land surface [*Yang and Lau*, 1998; *Kawamura*, 1998] play an additional role. *Zhang and Qian* [2000] noted the correlation between the SAH and Indian Ocean SST but did not trace the origin of this correlation to their common cause, ENSO.

3.2. Low-Level Circulation

[11] To examine the IOBM influence on surface climate, we construct warm-cold IOBM composites for precipitation, 850 hPa geopotential height and wind velocity (Figure 4). A total of 11 warm (1958, 1959, 1969, 1970, 1973, 1983, 1987, 1988, 1991, 1998, 2003) and 11 cold (1955, 1956, 1965, 1968, 1971, 1974, 1984, 1985, 1989, 1994, 2000) years are chosen when the Apr(1) IOBM index exceeds 0.75 and −0.75 standard deviation, respectively. Composites based on the Nov(0)-Jan(1) Nino3 index give similar results as the majority of warm IOBM events (8 out of 11) follow El Niño events defined earlier. Similarly, 8 of 11 cold IOBM events follow La Nina events.

[12] Summer precipitation increases over India and most of the tropical Indian Ocean (Figure 4). The associated condensational heating probably forces the Matsuno-Gill pattern in the upper troposphere (Figure 2b). The southwest monsoon increases over the Arabian Sea. The intensified Findlater jet is consistent with the SST cooling off the Somali coast (Figure 2b). Over the Indo-China Peninsular and South China Sea, the southwest monsoon weakens, as part of a large-scale anomalous anticyclone centered in the subtropical Northwest Pacific. The southerlies on the northwest flank of this anticyclone increase the moisture transport onto east China, increasing rainfall there. The easterly anomalies over the Maritime Continent are broadly consistent with the Kelvin wave response to increased rainfall over the tropical Indian Ocean.

4. Coupled Modeling

[13] To investigate to what extent the aforementioned anomaly patterns are due to the Indian Ocean warming, we use the Fast Ocean-Atmosphere Model (FOAM) version 1.5. The atmospheric component is a parallel version of the National Center for Atmospheric Research (NCAR) Community Climate Model (CCM) 2.0 with CCM3 physics, rhomboidal truncation at zonal wavenumber 15 (R15) in the horizontal and 19 sigma levels in the vertical. The ocean model is similar to the Geophysical Fluid Dynamics Laboratory (GFDL) Modular Ocean Model (MOM), with a resolution of 1.4° latitude × 2.8° longitude and 24 vertical levels. Without flux adjustment, the model has been run for more than a thousand years without major climate drifts. FOAM has been used to study climate variability both in and outside the tropics [*Liu et al.*, 2000; *Wu and Liu*, 2003].

[14] We carry out two sets of 50-member ensemble experiments initialized with positive and negative SST anomalies over the tropical Indian Ocean, respectively. Each member run is initialized on July 16 from a different year of a long control run. As the initial condition, temperature anomalies are prescribed as follows in the top 40 m the ocean model: zonally uniform from the African coast to 100°E and reduced to zero at 110°E. In the meridional direction, the anomalies are uniform from the Asian coast to 15°S and tapered to zero at 20°S. The maximum ocean temperature anomalies are set at 0.5°C for the positive and −0.5°C for the negative case. The ensemble mean is analyzed to isolate the coupled response to an initial warming and cooling over the tropical Indian Ocean. The results are similar between the positive and negative cases except a sign difference. For simplicity we show the positive minus negative case results for August in Figure 5, as in our observational analysis in Figure 4.

[15] The model captures the gross features of the observed anomalies associated with the IOBM documented in Section 3. While gradually decreasing in amplitude, the Indian Ocean warming persists for the next few months (not shown). In August, the positive SST anomalies cause an overall increase in precipitation over most of the Indian Ocean, which excites a Matsuno-Gill pattern in the upper tropospheric geopotential height (Figure 5a), with subtropical maxima west of 90°E and an equatorial maximum to the east indicative of the Rossby and Kelvin wave response, respectively. The SAH strengthens with height anomalies extending far into the west from South Asia to North Africa, much as in observations.

[16] The lower-level wind response is also similar to observations (Figure 5a versus Figure 4). The southwest monsoon strengthens over the Arabian Sea, reducing the initial warming off the Somali coast. The southwest monsoon weakens from Indo-China, through the South

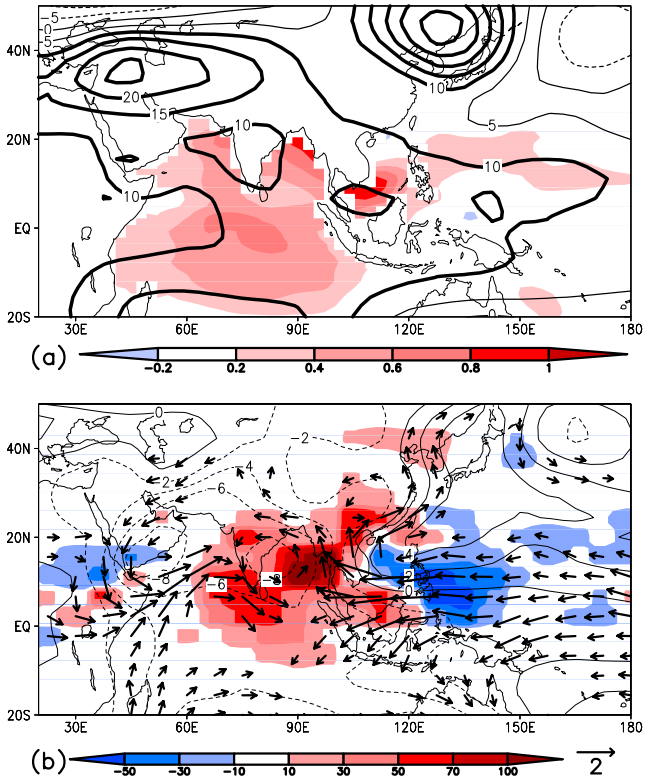

Figure 5. August ensemble-mean response of the coupled model to an initial warming in the top 40 m of the tropical Indian Ocean as represented by the positive-negative case difference: (a) SST (color in °C) and 200 hPa geopotential height (contours in m); (b) precipitation (color in mm/month), geopotential height (contours in m), and wind velocity (vectors in m s^{-1}) at 850 hPa.

China Sea, to the tropical West Pacific. In addition to an increase over India and the tropical Indian Ocean, rainfall decreases over much of the subtropical Northwest Pacific despite a weak increase in SST there, a remote response to Indian Ocean warming noted by *Annamalai et al.* [2005b] in their study of atmospheric response during Dec(0)–May(1). This rainfall decrease is associated with the development of a subtropical anticyclone to the north. Further to the north east of Japan, there are barotropic circulation anomalies (Figure 5b), possibly associated with the eastward propagation of a Rossby wave train [*Enomoto et al.*, 2003].

[17] The overall similarity between observations and the model simulation leads us to conclude that much of the following climatic anomalies observed in the summer subsequent to an El Niño event is due to the Indian Ocean warming of long persistence: the strengthened SAH in the upper troposphere, the strengthening and weakening of the southwest monsoon over the Arabian and South China Seas, [*Xie et al.*, 2003] respectively, and a low-level anomalous anticyclonic circulation over the subtropical Northwest Pacific [*Wang et al.*, 2003] that brings about rainfall anomalies over east China [*Huang et al.*, 2004]. *Kumar and Hoerling* [2003] and *Lau et al.* [2005] note a poleward shift in zonal-mean height anomalies in the upper troposphere on either side of the equator during the summer following an El Niño. Our results suggest that this poleward shift is a signature of the Rossby wave response as positive anomalies of SST and rainfall become confined to the tropical Indian Ocean from spring to summer.

5. Conclusions

[18] The IOBM is the dominant mode of Indian Ocean SST variability on interannual timescales. We have investigated the effects of this IOBM on atmospheric circulation and climate in the surrounding regions and how it helps prolong the influences of ENSO. Our observational analysis reveals a number of anomaly patterns associated with the IOBM, which are reproduced in a coupled model simulation initialized with a basin-wide warming in the tropical Indian Ocean mixed layer. Together, our observations and model results suggest the following capacitor mechanism for the IOBM to exert its influence. During its development and decay stages, El Niño forces the tropical Indian Ocean to warm up, like a battery charging a capacitor. Several issues remain: the mechanism for sustaining Indian Ocean SST anomalies through summer needs to be studied, and not all the IOBM events are induced by ENSO.

[19] This IOBM warming lags El Niño by about one season and peaks in late winter and early spring. While El Niño decays rapidly in spring and vanishes by summer, the IOBM warming persists through summer and unleashes its influence, like a discharging capacitor that sustains electric currents after the battery is switched off. *Annamalai et al.* [2005b] invoke a similar capacitor mechanism to explain the delayed onset of the South Asian summer monsoon following an El Niño but our results show that the Indian Ocean capacitor effect extends longer through the summer.

[20] This capacitor mechanism explains why climatic anomalies in some parts of the Indo-Pacific region are more robust in the summer following than concurrent with El Niño, despite much smaller and virtually vanishing Nino3 SST anomalies (−0.2 in Jul(1) vs. 1.4 standard deviation in Jul(0); Figure 1). The IOBM warming causes precipitation to increase over the tropical Indian Ocean, which forces a Matsuno-Gill pattern in the upper troposphere and strengthens the SAH. Near the ground, the southwest monsoon intensifies over the Arabian Sea and weakens over the South China Sea. The intensified Findlater jet is a negative feedback to the IOBM, cooling the western Arabian Sea via coastal upwelling. Over the subtropical Northwest Pacific, an anomalous anticyclone forms in the lower troposphere, associated with a local reduction in precipitation that our model simulation suggests is a remote response to the Indian Ocean warming.

[21] Thus, the IOBM is not just a passive response to ENSO but an important predictor for summer climate unleashing its influence after the equatorial Pacific has returned to normal. The IOBM is generally well simulated in coupled general circulation models [*Saji et al.*, 2006] and predictable at a six-month or longer lead [*Luo et al.*, 2005]. While pointing to the capacitor effect of the Indian Ocean, our results do not exclude the possibility that land surface processes and the Atlantic make contribute to the delayed response in summer to a preceding and dissipated El Niño. In fact, for a successful seasonal prediction for an individual summer, it is probably important to initialize dynamical

models with anomalies both in and outside the tropical Indian Ocean given the modest amplitudes of the IOBM.

[22] **Acknowledgments.** We wish to thank R. Lu for helpful discussion, Wu Shu and Li Chun for assistance in setting up the model experiments, and anonymous reviewers for useful comments. This work is supported by the Natural Science Foundation of China 40676010, the Ocean University of China Green Card Project, and the Japan Agency for Marine and Earth Science and Technology. IPRC publication 426 and SOEST publication 7072, and CCR contribution 918. All simulations are carried in the High Performance Computer Center of Ocean University of China.

References

Annamalai, H., S.-P. Xie, J.-P. McCreary, and R. Murtugudde (2005a), Impact of Indian Ocean sea surface temperature on developing El Niño, *J. Clim.*, *18*, 302–319.

Annamalai, H., P. Liu, and S.-P. Xie (2005b), Southwest Indian Ocean SST variability: Its local effect and remote influence on Asian monsoons, *J. Clim.*, *18*, 4150–4167.

Enomoto, T., B. J. Hoskins, and Y. Matsuda (2003), The formation mechanism of the Bonin high in August, *Q. J. R. Meteorol. Soc.*, *129*, 157–178.

Gill, A. E. (1980), Some simple solutions for heat-induced tropical circulation, *Q. J. R. Meteorol. Soc.*, *106*, 447–462.

Huang, R., G. Huang, and Z. Wei (2004), Climate variations of the summer monsoon over China, in *East Asian Monsoon*, edited by C. P. Chang, pp. 213–270, World Sci., Hackensack, N. J.

Kawamura, R. (1998), A possible mechanism of the Asian summer monsoon-ENSO coupling, *J. Meteorol. Soc. Jpn.*, *76*, 1009–1027.

Klein, S. A., B. J. Soden, and N.-C. Lau (1999), Remote sea surface temperature variations during ENSO: Evidence for a tropical atmospheric bridge, *J. Clim.*, *12*, 917–932.

Kug, J., T. Li, S. An, I. Kang, J. Luo, S. Masson, and T. Yamagata (2006), Role of the ENSO–Indian Ocean coupling on ENSO variability in a coupled GCM, *Geophys. Res. Lett.*, *33*, L09710, doi:10.1029/2005GL024916.

Kumar, A., and M. Hoerling (2003), The nature and causes for the delayed atmospheric response to El Niño, *J. Clim.*, *16*, 1391–1403.

Lau, N.-C., A. Leetmaa, M. J. Nath, and H.-L. Wang (2005), Influences of ENSO-induced Indo-Western Pacific SST anomalies on extratropical atmospheric variability during the boreal summer, *J. Clim.*, *18*, 2922–2942.

Liu, X., Z. Liu, J. E. Kutzbach, S. C. Clemens, and W. L. Prell (2006), Hemispheric insolation forcing of the Indian Ocean and Asian monsoon: Local versus remote impacts, *J. Clim.*, *19*, 6195–6208.

Liu, Z., J. Kutzbach, and L. Wu (2000), Modeling climate shift of El Niño variability in the Holocene, *Geophys. Res. Lett.*, *27*(15), 2265–2268.

Luo, J.-J., S. Masson, S. Behera, S. Shingu, and T. Yamagata (2005), Seasonal climate predictability in a coupled OAGCM using a different approach for ensemble forecasts, *J. Clim.*, *18*, 4474–4497.

Reason, C. J. C., R. J. Allan, J. A. Lindesay, and T. J. Ansell (2000), ENSO and climatic signals across the Indian Ocean basin in the global context: Part I. Interannual composite patterns., *Int. J. Climatol.*, *20*, 1285–1327.

Saji, N. H., S.-P. Xie, and T. Yamagata (2006), Tropical Indian Ocean variability in the IPCC 20th-century climate simulations, *J. Clim.*, *19*, 4397–4417.

Wang, B., R. Wu, and T. Li (2003), Atmosphere-warm ocean interaction and its impact on Asian-Australian monsoon variability, *J. Clim.*, *16*, 1195–1211.

Wu, L., and Z. Liu (2003), Decadal variability in the North Pacific: The eastern North Pacific mode, *J. Clim.*, *16*, 3111–3131.

Wu, R., and B. Kirtman (2004), Understanding the impacts of the Indian Ocean on ENSO variability in a coupled GCM, *J. Clim.*, *17*, 4019–4031.

Xie, S.-P., H. Annamalai, F. A. Schott, and J. P. McCreary (2002), Structure and mechanisms of south Indian Ocean climate variability, *J. Clim.*, *15*, 864–878.

Xie, S.-P., Q. Xie, D. Wang, and W. T. Liu (2003), Summer upwelling in the South China Sea and its role in regional climate variations, *J. Geophys. Res.*, *108*(C8), 3261, doi:10.1029/2003JC001867.

Yang, S., and K.-M. Lau (1998), Influences of sea surface temperature and ground wetness on Asian summer monsoon, *J. Clim.*, *11*, 3230–3246.

Zhang, Q., and Y. Qian (2000), Interannual and interdecadal variations of the South Asian High, *Chin. J. Atmos. Sci.*, *24*, 67–78.

Q. Liu, L. Wu, and J. Yang, Physical Oceanography Laboratory, Ocean University of China, Qingdao 266003, China. (qdycjl@ouc.edu.cn)

Z. Liu, Center for Climatic Research, University of Wisconsin, Madison, WI 53706, USA.

S.-P. Xie, IPRC/SOEST, University of Hawaii, Honolulu, HI 96822, USA. (xie@hawaii.edu)